실크 피브로인의 마이크로 플루이딕 디바이스 개발 및 응용

Chung-Ang University, Da Vinci College of General Education
OK JA Yoon

1. 서론

✓ 실크 피브로인의 마이크로 플루이딕 디바이스 개발 및 응용[1,2]

- 최근 많은 연구가 보고되고 있는 마이크로 플루이딕 디바이스(microfluidic reaction system)는 수십에서 수백 마이크로 미터의 채널 크기를 가지는 장치로 이를 이용하여 화학 물질, 나노 소재, 재료 합성, 바이오 물질 분석 등 다양한 연구분야에 활용되고 있음.

- 마이크로 플루이딕 디바이스는 소량의 시약을 사용하여 반응 시간의 단축, 빠른 물질 및 열 전달, 확산 거리 최소화, 부 반응(side reaction)의 최소화 등 다양한 장점을 가지고 있음.

- 마이크로 플루이딕 시스템의 기본 소자: 마이크로 밸브, 마이크로 펌프

- 마이크로 플루이딕 시스템의 제작 기술: 미세제작법, 결질 미세 가공, 연질미세가공

2. 연구 동향

✓ **Silk-Microfluidics for advanced biotechnological applications: A progressive review[3]**

- 거미나 누에코치에서 추출한 실크 피브로인은 재생 의학 분야나 뿐만 아니라 최근 lab-on-a–chip 응용 분야에 많이 보고되고 있음. 실크의 biosppining은 자연에 가까운 미세 유동 장치(microfluidic-maneuver)에 사용되고 있음.

- 다공성 실크 지지체(scaffolds) 내의 미세 유체 채널 네트워크는 조직 공학 응용 분야에서 혈관 형성을 위한 전구체 역할을 하는 것 외에도 영양분과 산소 공급의 최적화 됨을 보고함.

- 천연 실크 섬유의 고유한 topographical features와 표면 친수성은 혈액 투석 및 화학적 센싱을 위한 효과적 장치의 개발에 매우 간단하고 저비용으로 기술적 개발을 제시하고 있음.

- Silk based biodegradable microfluidic platforms은 환경 독성 평가나 인체내의 체액에서 대사 물질의 간단한 평가하기 위한 플랫폼으로 엄청난 가능성과 기술적 전망을 제시하고 있음.

- 이 리뷰논문은 거미나 누에코치에서 추출한 실크 피브로인을 이용한 silk-microfluidics의 영역에서의 최근 연구 동향과 개발을 보고하고 있음.

- **최근 silk-microfluidic 기술의 응용**

- Water collection:실크 파이버 위에 응집된 water droplet은 spindle-knots의 형태를 이루고 있으며 이러한 물성은 표면의 거칠기 향상과 표면의 wettability와 같은 물성의 변화등을 보고함.

- Blood typing:

- Drug delivery:

- Bio/chemo sensors:

- Cell culture and micro-channeled biomaterials:

- In situ evaluation of chemoembolization agent:

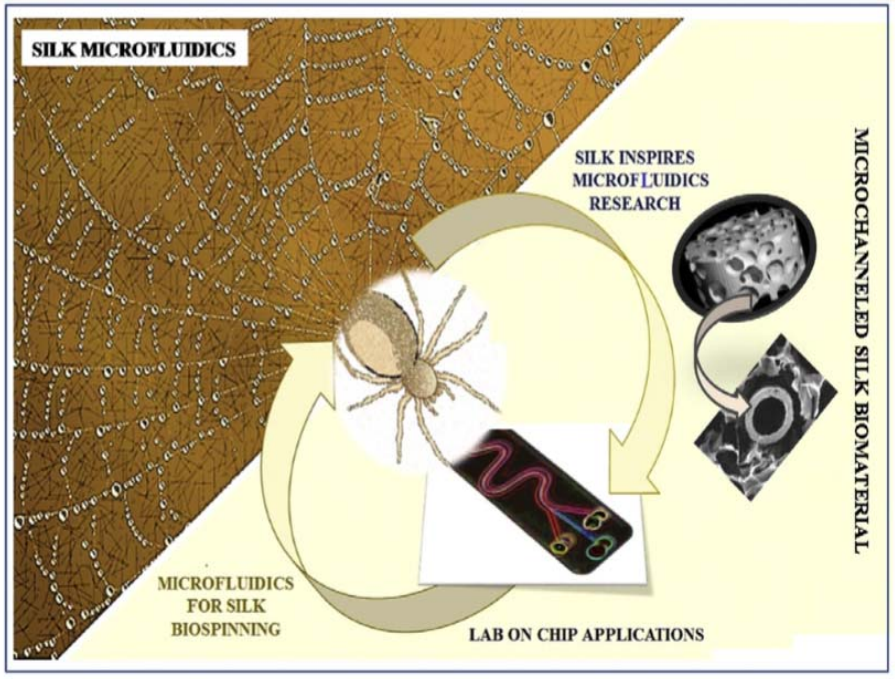

Fig. 1.Concept of silk-microfluidics

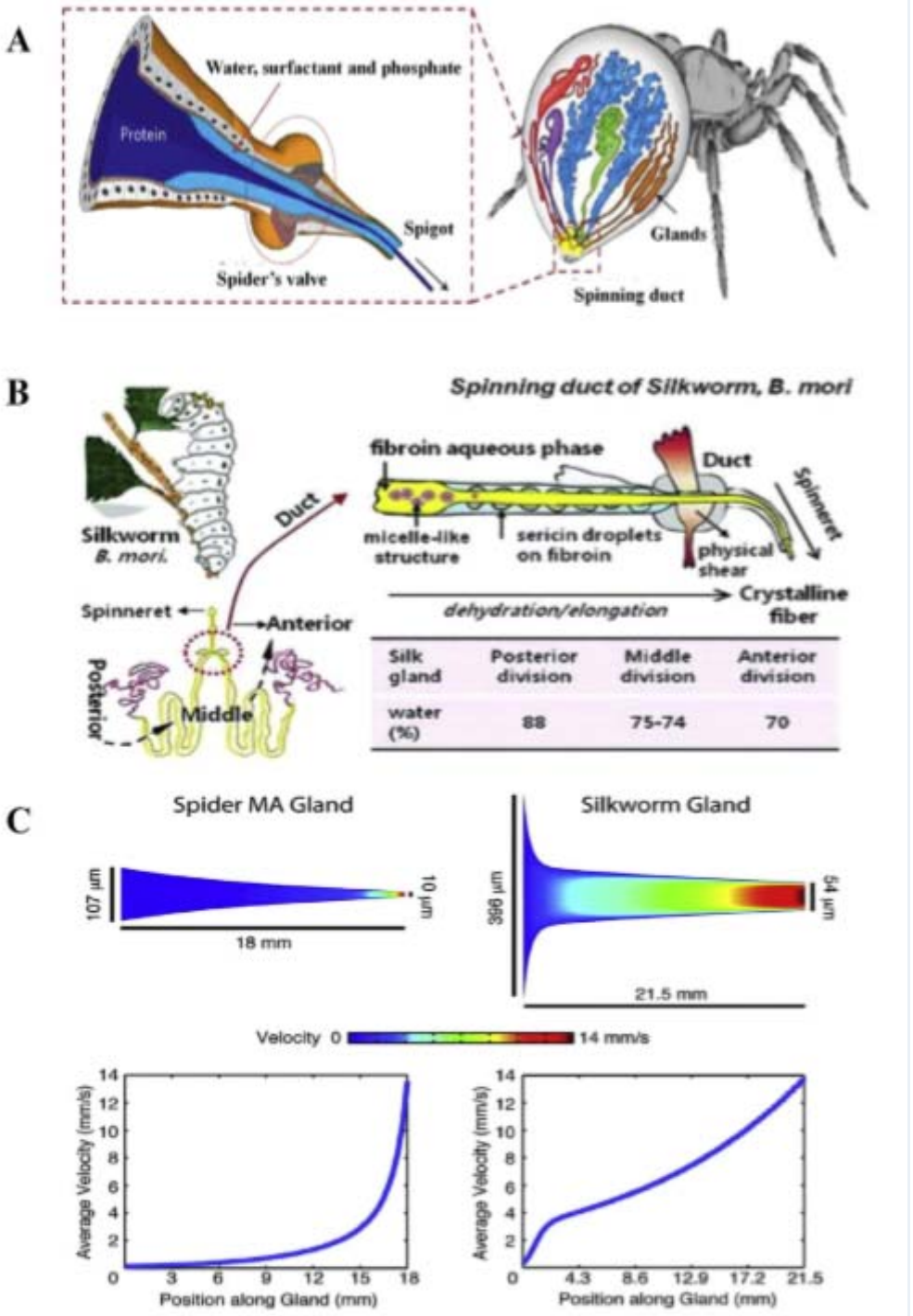

Fig.2. (A) Anatomy of the silk-spinning system of spiders. Reproduced from (Kangetal., 2011) with permission.©2011MacmillanPublishers Limited. (B) Illustration of a silkworm's duct spinning . Reproduced from (Chaeetal.,2013)with permission. ©2013 WILEY-VCH Verlag GmbH & Co. KGaA, Weinheim. (C) Magnitude of the velocity vector (top) and cross-sectionally averaged to talvelocity (bottom) along the MA silk gland of the spider (left) and silkworm silk gland (right). Reproduced from (Breslaueretal.,2009) with permission. ©2009 American Chemical Society.

- **Water collection: 3D 지지체로 응용하기 위하여 실크 파이버 위에 응집된 water droplet은 spindle-knots의 형태를 이루고 있으며 이러한 물성은 표면의 거칠기 향상과 표면의 wettability와 같은 물성의 변화 등을 보고함.**

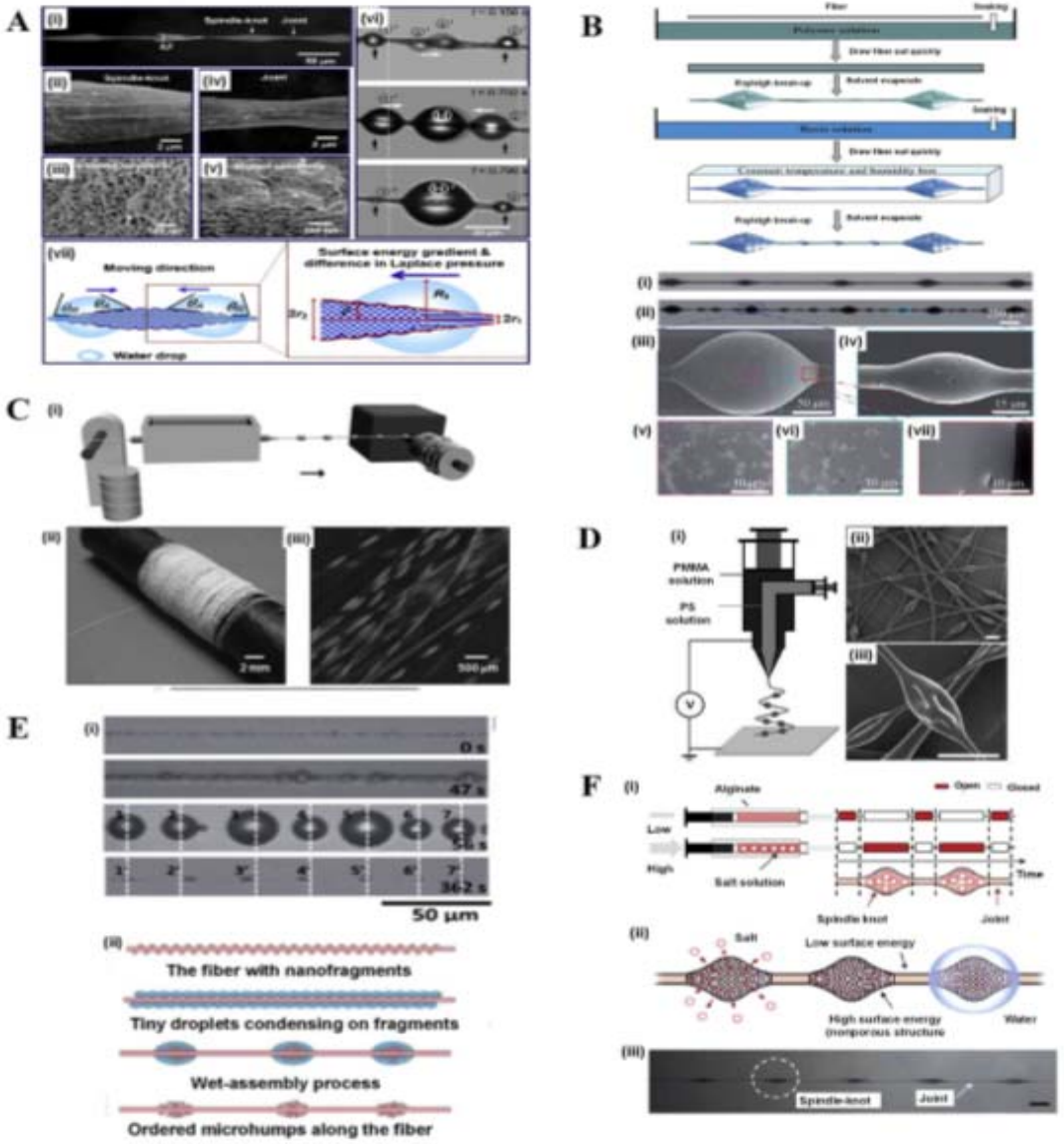

Fig.3. (A) Microstructures of spider silk and directional transport of water droplets on it. (i) The wet-rebuilt spider silk is composed of (ii, iii) periodic spindle-knots with random nanofribrils and (iv, v) joints with aligned nanofribrils. (vi) Directional transport of water droplets on the spider silk. Tiny water droplets move from joints towards knots. (vii) Mechanism of the directional transport of water droplets. Reproduced from (Juetal.,2014) with permission (B) Scheme of fabricating bio-inspired fibers with multi-gradient and multi-scale spindle knots. Structural features of the bioinspired fiber prepared by dip coating technique. (i and ii) Optical images showing periodic spindle knots on the fiber surface and some small spindle knots between the two larger ones. (iii–vi) Scanning electron microscope (SEM) images of larger and smaller spindle knots. (v, vi and vii) Surface of larger spindle knot at different areas. Reproduced from (Hou et al., 2012) with permission. (C) (i) Schematic illustration of the fluid coating method used for the large-scale fabrication of bioinspired fibers. (ii, iii) Optical images of the as-prepared bioinspired fibers with periodic spindle-knots. Reproduced from (Bai et al., 2011) with permission. (D) (i) Coaxial electrospinning using diluted poly(methylmethacrylate)(PMMA) solution (outer) and concentrated polystyrene(PS) solution(inner). When the two solutions are pumped out from injectors, inner PS solution is stretched by electrostatic force and forms the PS fiber, while the dilute PMMA solution adhering to the PS fiber contracts to spindle-knots. (ii, iii) SEM images of the electrospun knotted microfibers.(scale bars=10μm). Reproduced from(Dongetal.,2012). (E) (i) In situ optical observation of bioinspired wet-assembly micro humps fiber (BWMF) formation. (ii) Illustration of the BWMF formation. Reproduced from (Song et al., 2014) (F) (i) Schematic of a digital control scheme for generating artificial spindle-knots and joints by means of topography modulation and nanoporous structure coding. (ii) Schematic of a fiber with a different surface energy and water-collection mechanism. (iii) Artificially spun fibers with spindle-knots and joints. Reproduced from (Kang et al., 2011)

- **누에 biospinning을 모방하기 위한 마이크로 플루이딕 장치**

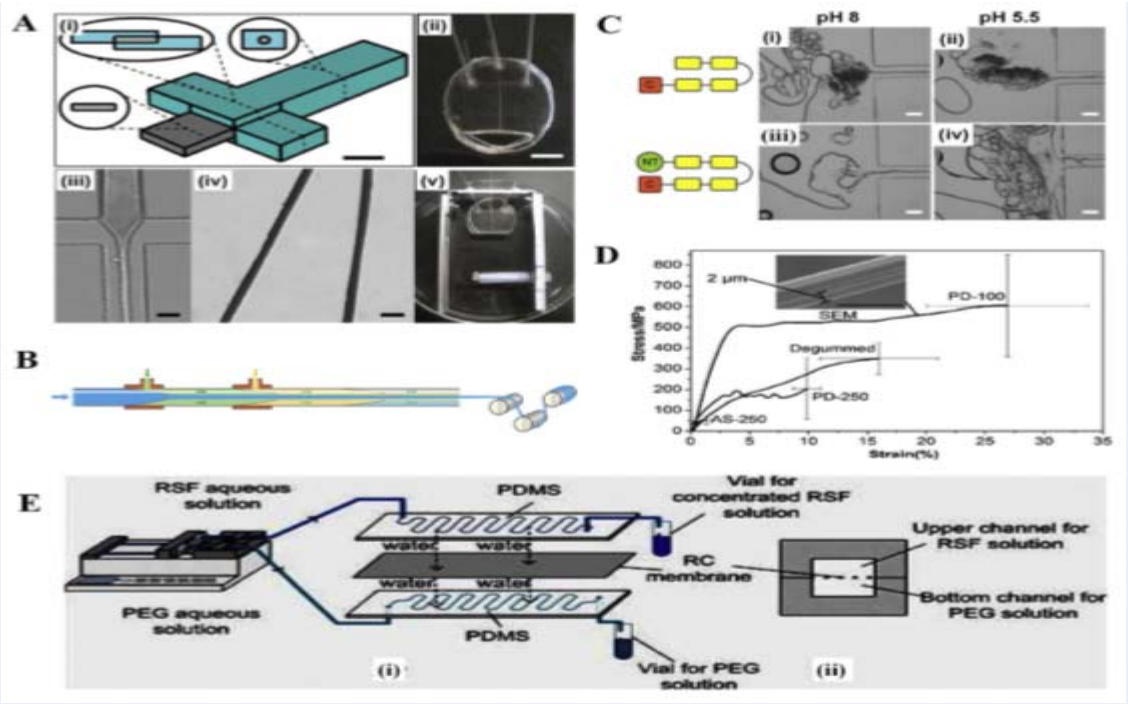

Fig. 4. (A) Microfluidic device design and fiber fabrication mimicking silkworm biospinning. (i) Schematic of the channel with selected cross sections illustrates 3-D multilayer design. (ii) The device, fabricated from poly(dimethylsiloxane) (PDMS), has three inlets (tubing attached for fluid transfer) and one outlet into a reservoir. (iii) Flow in the device during use illustrates the hydrodynamic focusing of the silk solution stream at the cross intersection. (iv) Regenerated silk fibroin (RSF) fibers fabricated in the device have smooth surfaces and consistent diameters. (v) A frame with an adjustable rod is used to aid in fiber collection. Reproduced from (Kinahan et al.,2011) with permission. ©2011 American Chemical Society. (B)A schematic biomimetic spinning device. A highly concentrated aqueous spidroin solution (blue) is pumped into a series of pulled glass capillaries. Aqueous buffers (green and yellow) are serially introduced into the device and form laminar flows that cause increased flow rate and shearing of the spidroin solution (i.e., the jet get sthinner).The laminar flow will allow for diffusion across the solution interfaces, which will lead to a gradual lowering of pH and elevation of pCO_2 in the spidroin solution when it travels through the device. Reproduced from (Rising and Johansson, 2015) with permission. ©2015 Nature America, Inc. (C) Investigation of the pH-relay role of NT in a spinning setting. The partial spidroin 4RepCT (lacking the pH-switch domain NT) form similar fiber sheets at pH 8 (i) as well as at pH 5.5 (ii). Inclusion of the pH-switch domain NT to yield the more complete mini-spidroin NT4ReCT almost inhibits fiber formation at pH 8 (iii). On the other hand, the pH-switching NT-domain induces striking amounts of fiber formation at pH 5.5 (iv). Reproduced from (Renberg and Andersson-Svahn, 2014) with permission. ©2014 Elsevier B.V. (D) Stress–strain curves of degummed cocoon silk, as-spun RSF fiber of AS-250, post-drawn RSF fibers of PD-250 and PD-100. (Scale bar=10μm). Reproduced from(Luoetal.,2014) with permission. ©2014ElsevierB.V. (E) Schematics of (i)experiments set up of co-current flow and (ii) cross sectional view of microfluidic channels for the donor solution and the acceptor solution. Reproduced from (Luoetal., 2012) with permission. ©2011Elsevier B.V.

- **SR-SAXS를 이용하여 마이크로 플루이딕 장치 안애서 실크 피브로인 용액의 응집 현상과 파이버 형성 과정 관찰.**

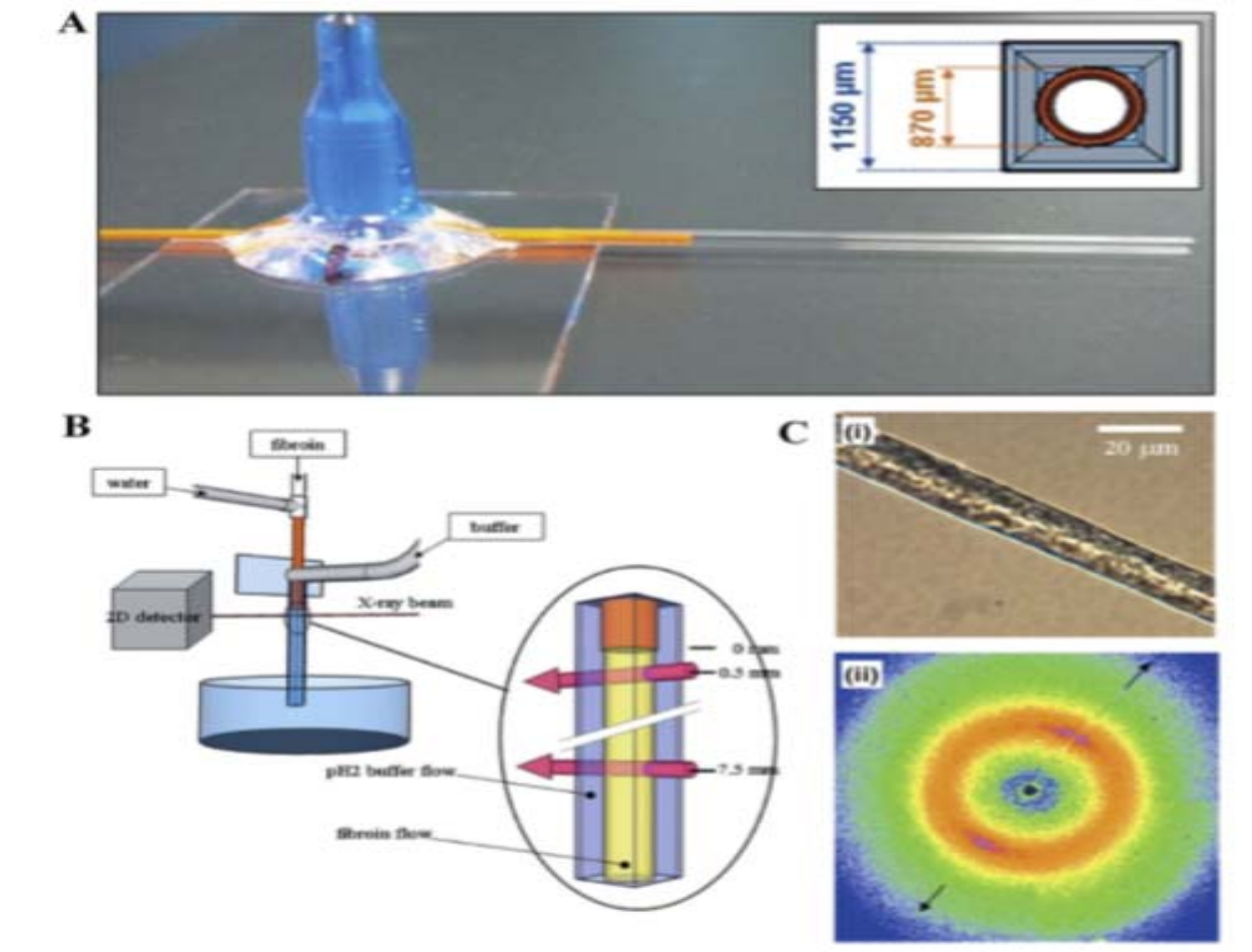

Fig.5. (A) Schematic design of a tube-in-square-pipe microfluidic cell. The inset shows the cross section of the two tubes. (B) Schematic set up of a microfluidic cell used for synchrotron radiation scattering experiments. The inset shows a zoom of the mixing zone and the positions millimeters from the inner capillary exit probed by the beam. (C) (i) Microscopic image of artificial silk. (ii) µ-Wide-angle X-ray scattering (µ-WAXS) pattern of artificial silk. The orientation of the equator is indicated by arrows. Reproduced from (Martel et al., 2008) with permission. ©2008 American Institute of Physics.

- **Coded fiber를 만들기 위한 마이크로 플루이딕 스피닝 칩**

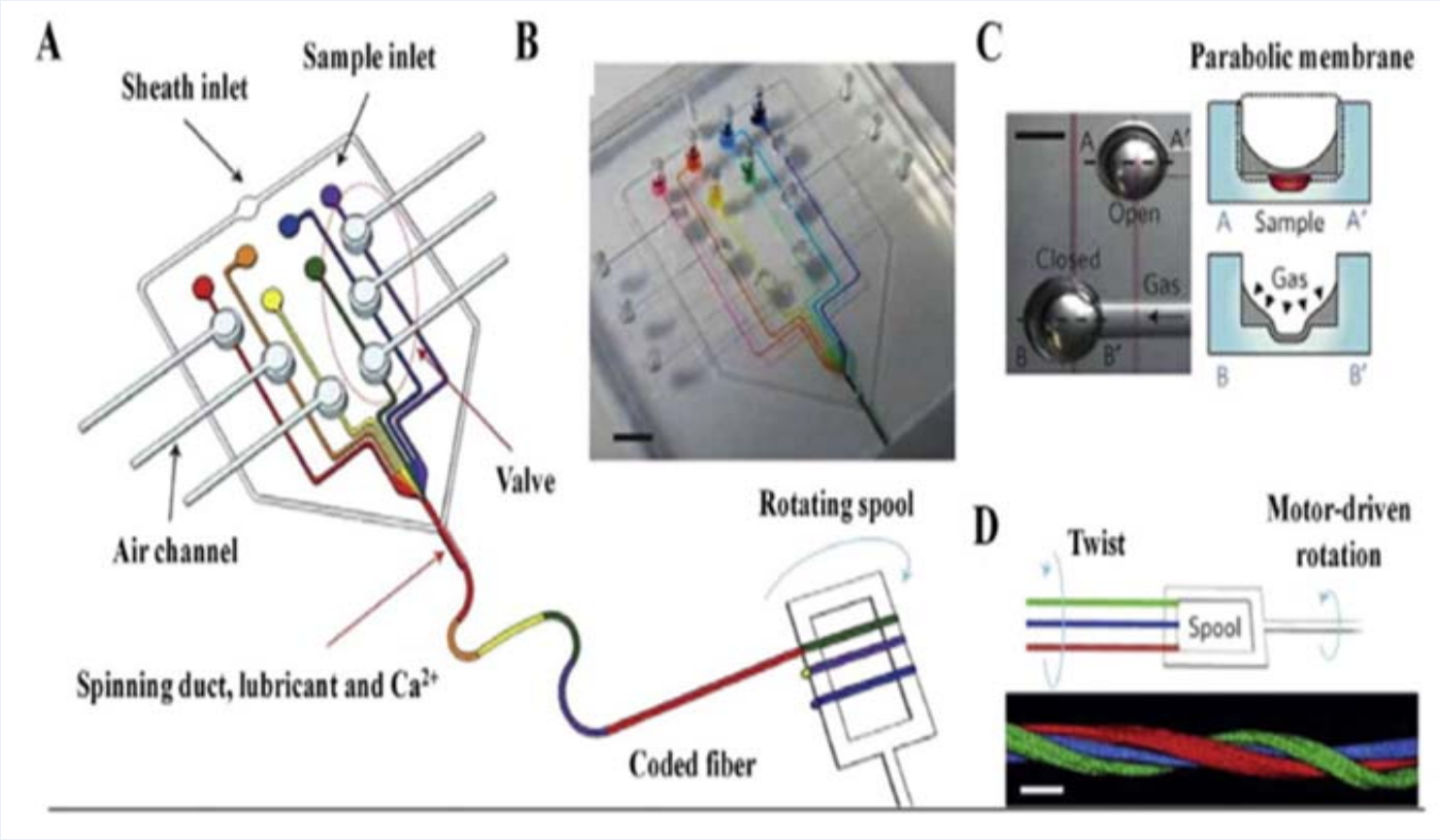

Fig. 6. (A) Conceptual description of the process of generating coded fibers. The extruded fibers were continuously wound on the spool by a motorized system. (B) Photograph of the microfluidic spinning chip. (C) Optical image of the 'open' and 'closed' states of the valve above the channel (left) and a cross-sectional schematic of the valve operation (right). (D) Schematic of the process of twisting fibers using a motor system (top) and a fluorescence micrograph of a twisted fiber with red-green-and blue-stained fibers. Reproduced from (Kangetal., 2011) with permission. ©2011Macmillan Publishers Limited.

- **실크로 만든 실을 이용한 Blood typing 방법**

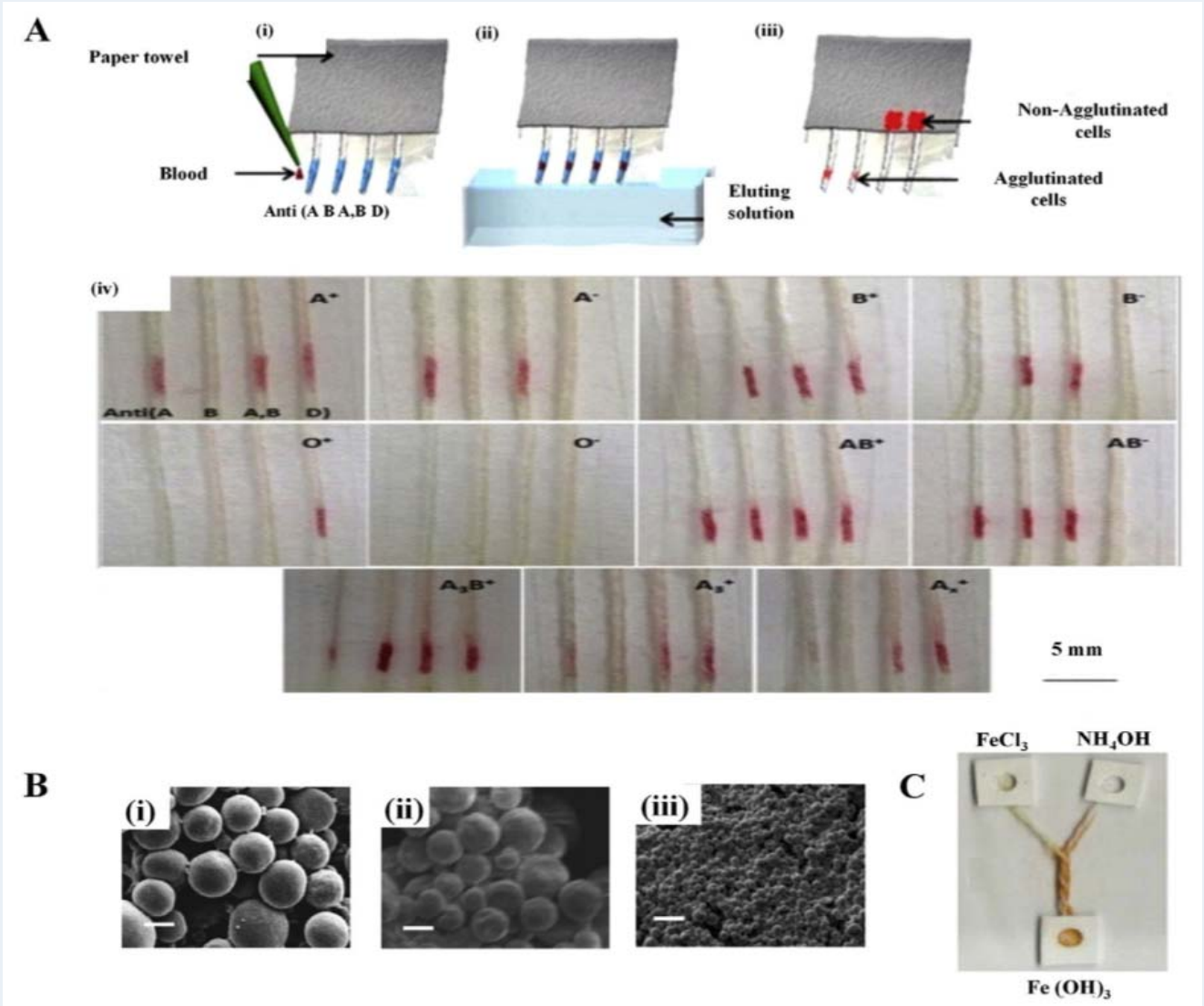

Fig.7. (A) Schematic diagram showing (i-iii) the blood typing method on thread. (i) Blood typing antibody (anti-A, anti-B, anti-A,B, and anti-D) and whole blood sample were deposited on each thread before (ii) eluting with buffer. (iii) Positive and negative results after elution. Images of ABO blood typing and its weak subgroups on (iv) silk threads. Reproduced from (Nilghaz etal.,2014) with permission. ©2014 American Chemical Society. (B) SEM images of silk spheres synthesized by changing silk concentrations: (i) 60mg ml^{-1}, (ii) 30$mgml^{-1}$, and (iii) 10$mgml^{-1}$ concentration. Reproduced from (Mitropoulosetal.,2014) with permission. ©2013WILEY-VCHVerlag GmbH & Co. KGaA, Weinheim. (C) Colorimetric detection of ferric hydroxide in Y-reactors. Synthesis of ferric hydroxide using acidulated ferric chloride in a silk device. The brown color of ferric hydroxide can be seen in the product reservoir. Reproduced from (Banerjeeetal.,2013) with permission. ©2013 Elsevier Ltd

- **Cell culture and micro-channeled biomaterials: Bio-microelectrical mechanical system (BioMEMS)로 이용하기 위한 silk based microfluidic device/channel**

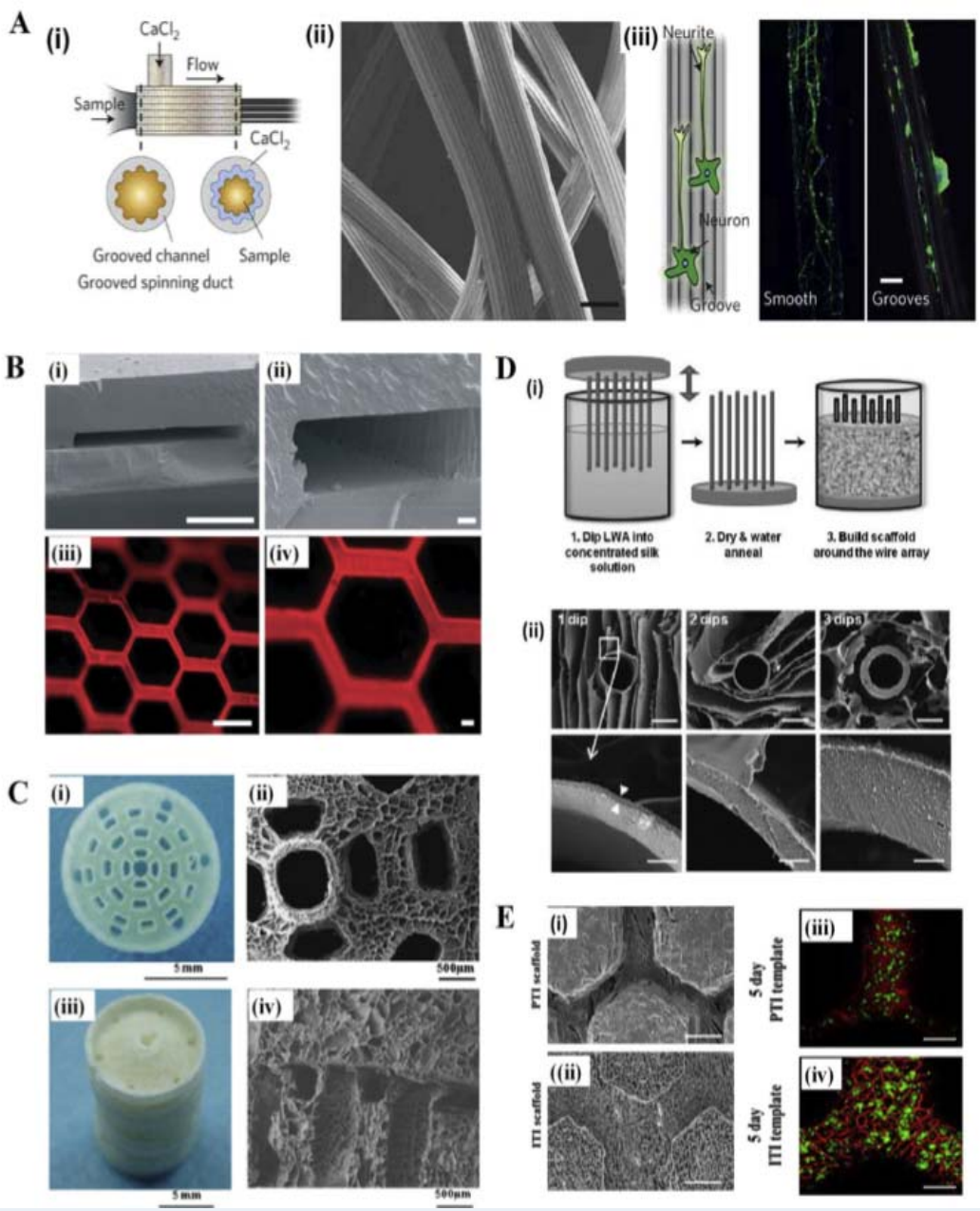

Fig.8. (A) (i) Schematic of groove coding on the fiber surface using a grooved round channel, (ii) Grooved fibers fabricated using the spinning chip, (iii) Schematic of neuron alignment on a grooved fiber (left) and fluorescence micrograph of neurons on a fiber without grooves(middle) and on a grooved fiber (right) (green, neuro filament; blue, nucleus). Reproduced from (Kangetal., 2011) with permission. ©2011Macmillan Publishers Limited. (B) Silk fibroin-based microfluidic devices. SEM images of the cross-sections of devices fabricated demonstrate retention of feature geometries in thin films with microchannel widths of approximately (i) 240 μm and (ii) 90μm. (iii, iv) Patent microfluidic devices are demonstrated by fluorescent micrographs of devices perfused with rhodamine solution. Retention of the perfusate within the microchannels suggests robust bonding at the interface. Reproduced from (Bettingeret al., 2007) with permission. ©2007WILEY-VCHVerlag GmbH & Co.K GaA, Weinheim . (C) Bottom-up generation of 3D microfluidic silk fibroin-gelatin (SF–G)scaffolds. (i) Monolayer scaffold has (ii) predefined microfluidic channels (iii) 3D assembled scaffolds, (iv) SEM images of predefined microfluidic channels in 3D. Reproduced from (Heetal.,2012) with permission.©2012 Elsevier Ltd. (D) Hollow channels lined with silk tubes. Depicted is a schematic of the LWA dipping process and subsequent scaffold fabrication. (ii) SEM micrographs of tubes formed by 1, 3 and 5 dips respectively. Reproduced from (Wray etal.,2012) with permission.©2012Elsevier Ltd. (E) (i, ii) SEM characterization of cellular morphology on the surface of PTI and ITI scaffold after5 d of culture (iii-iv) Cells distributed indifferent regions of PTI and ITI scaffolds at day 5.

- **In situ evaluation of chemoembolization agent: 마이크로 플루이딕 장치를 이용하여 embolic agent로 사용할 수 있는 silk – elastin like protein polymer (SELPs) 개발**

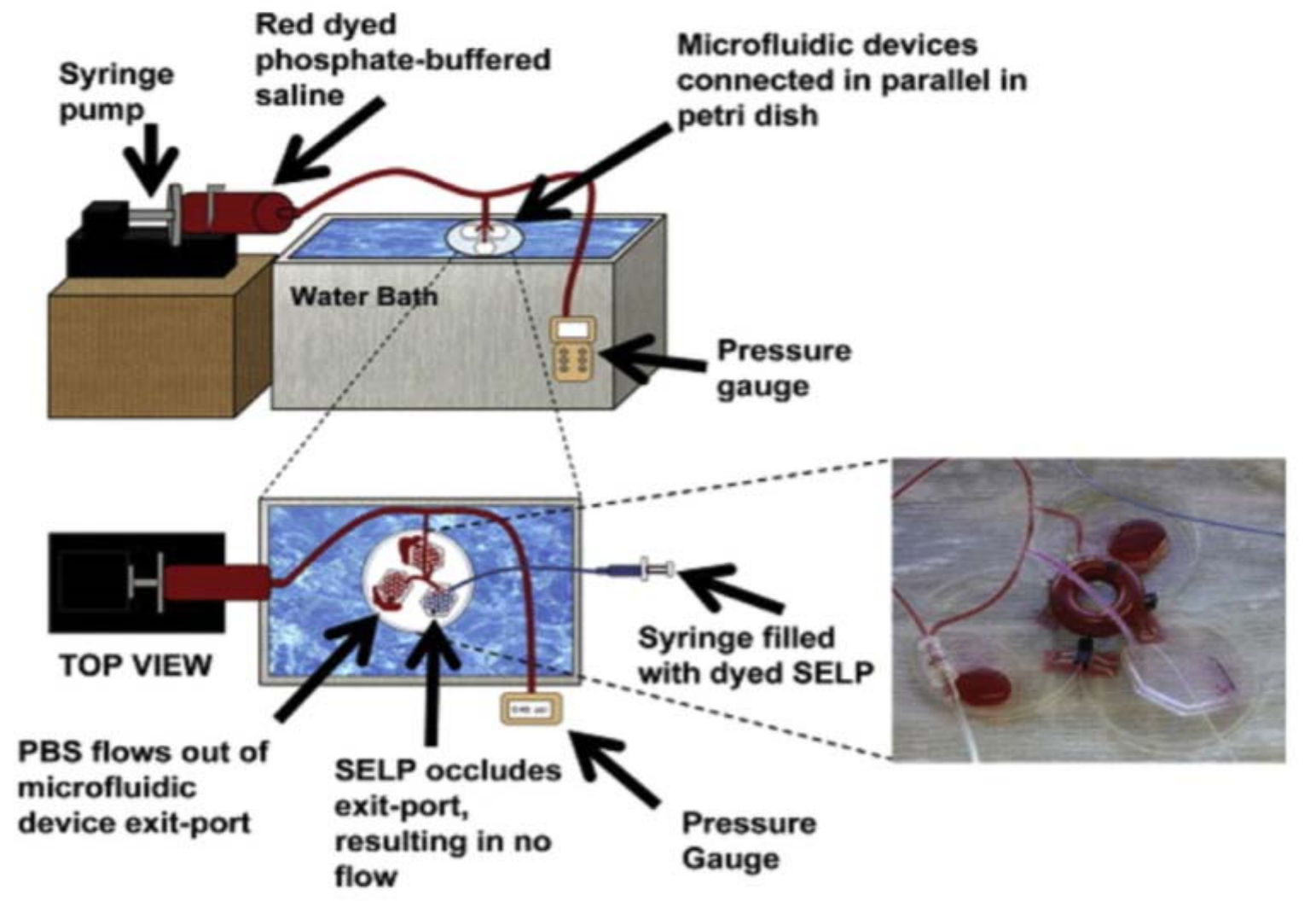

Fig.9. Schematic of the in vitro test set up. Set up used to evaluate the occlusive ability of the c and I date formulation under flow conditions. The image shows occlusion of the microfluidics device by 12%w/w sheared SELP-815 K. Reproduced from (Poursaidet al., 2015) with permission. ©2015 Elsevier Ltd.

✓ Silk Fibroin Microfluidic Device[4]

- 바이오 메디컬 응용 분야의 연구 동향은 약물 전달, 진단, 조직 공학 등의 기술을 개선하기 위해 미세 제작 시스템의 설계 및 개발을 BioMEMS (Bio-microelectrical mechanical systems)라고 불리는 마이크론 길이 스케일을 특징으로 하는 기술과 세포 또는 단일 생체 분자와 같은 생물 시스템과 상호 작용할 수 있는 시스템 개발을 보고하고 있음.

- BioMEMS를 개발하기 위한 전략은 전형적으로 전통적인 미세 가공 재료 및 공정을 적용하여 실리콘 및 폴리 디메틸 실록산 (PDMS)을 포함하는 비 분해성 물질을 사용하여 제조 된 시스템을 만들었으나 최근 연구는 생분해성 고분자를 사용하여 이식 가능한 BioMEMS가 약물 전달 시스템이나 조직 공학과 같은 생체 내에 적용 가능하도록 보고하고 있음.

- BioMEMS 장치는 젤라틴, 알긴산 염, 폴리 (L- 락트산) (PLA), 폴리 (L- 락트산) (PLGA), 폴리 (글리세롤 - 코 - 세바 케이트) (PGS) 등이 보고되고 있으며 재료 특성 관점에서 BioMEMS 제작을 위한 이상적인 생체 재료의 특징은 다음과 같음.
  단백질 또는 성장 인자 결합을 촉진하기 위한 조건을 만족, 세포의 부착과 증식을 촉진, 표면의 잠재적인 화학적 변형 가능, 기능화를 이용하여 이식 장치의 지속 기간을 최대화하기 위한 분해 속도 조절 가능, 견고하면서 유연성 있는 기계적 특성, 비교적 저렴하여야 함.

- Bombyx mori 누에에서 추출한 실크 피브로인 단백질은 FDA 승인을 받았으며 수술, 약물 전달, 조직 공학 등 다양한 용도로 의학에 응용 되고 있음. 실크 피브로인은 in vitro 및 in vivo biocompatibility , 높은 기계적 성질, 상대적으로 느린 분해성 단백질의 특성을 가짐

- **아날로그 - 리소그래피 기술과 같은 프로세스를 개발하여 실크 피브로인 micromolding과 device를 개발함.**
- **독성 용액이나 거친 가공을 피한고 재생 된 실크 피브로인 용액의 몰딩 방벙을 이용하여 미세 제작 된 실크 필름을 제조함.**
- **Microfluidic device는 물에 안정한 실크 피브로인 막을 적층하여 제조하여 장치의 생체 적합성 및 기능성을 human hepato carcinoma cellline를 최대 5 일 동안 배양 한 결과 silk fibroin-based microfluidic devices에서 배양된 간세포는 잘 배양됨.**

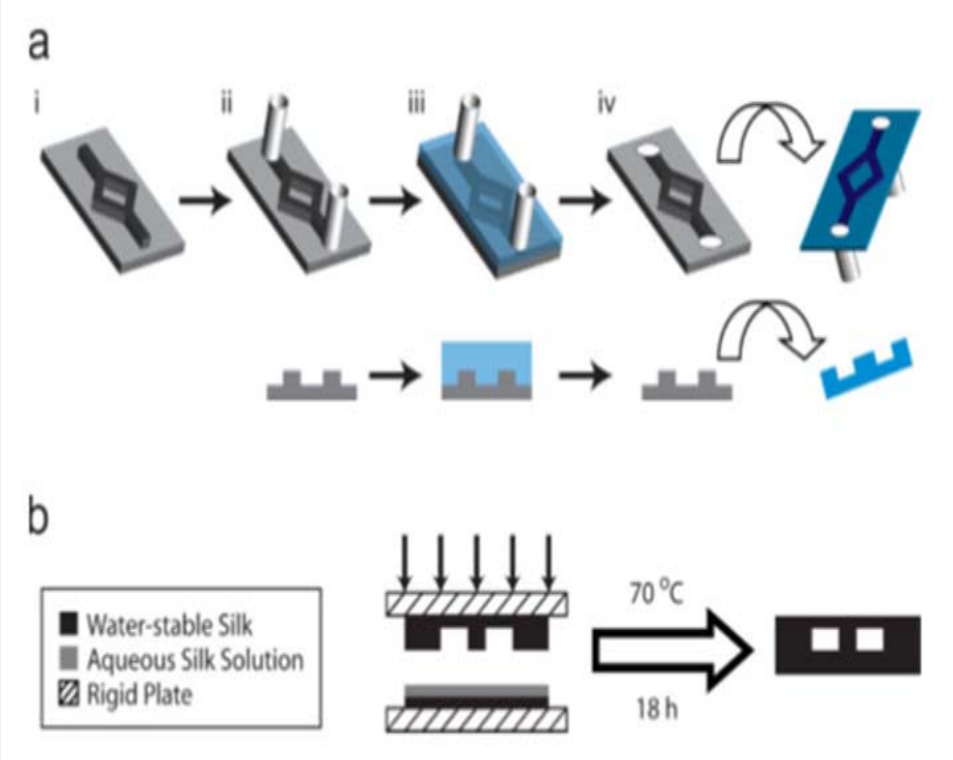

Figure 1. Fabrication Strategy for Silk Fibroin Microfluidic Devices. a) The process flow is diagrammed in both an isometric view and a cross-sectional view through the midline (i) through the successive steps of the process. PDMS negative molds (i) are fabricated using traditional soft lithography techniques (not shown). PDMS molds are modified with silicone tubing (ii) prior to solvent casting of aqueous silk fibroin solution (iii). Upon water evaporation, micromolded films are delaminated with integrated macroscopic fluidic connections (iv). Both micromolded and flat silk films are treated with aqueous methanol solutions (see text). b) Final assembly of silk microfluidic devices was performed by bonding appropriate water-stable silk fibroin layers using additional regenerated aqueous silk fibroin solution. Layers are bound between rigid plates under mechanical pressure at 70°C for 18 h to produce a water-insoluble silk fibroin interface with increased b-sheet content (see text)

		Young's Modulus [MPa]	UTS [MPa]	Elongation at Break [%]	Toughness Modulus [MJ/m^3]
PGS	(n=8)	1.72 ± 0.79	0.281 ± 0.13	19.8 ± 1.11	0.0294 ± 0.0146
Silk Fibroin	(n=5)	107.63 ± 18.29	7.60 ± 0.51	20.9 ± 0.16	1.21 ± 0.0118

Table 1. Comparison of Mechanical Properties of Regenerated Silk Fibroin and PGS Films. The value n represents the number of samples in each dataset. Data reported as mean±s.d.

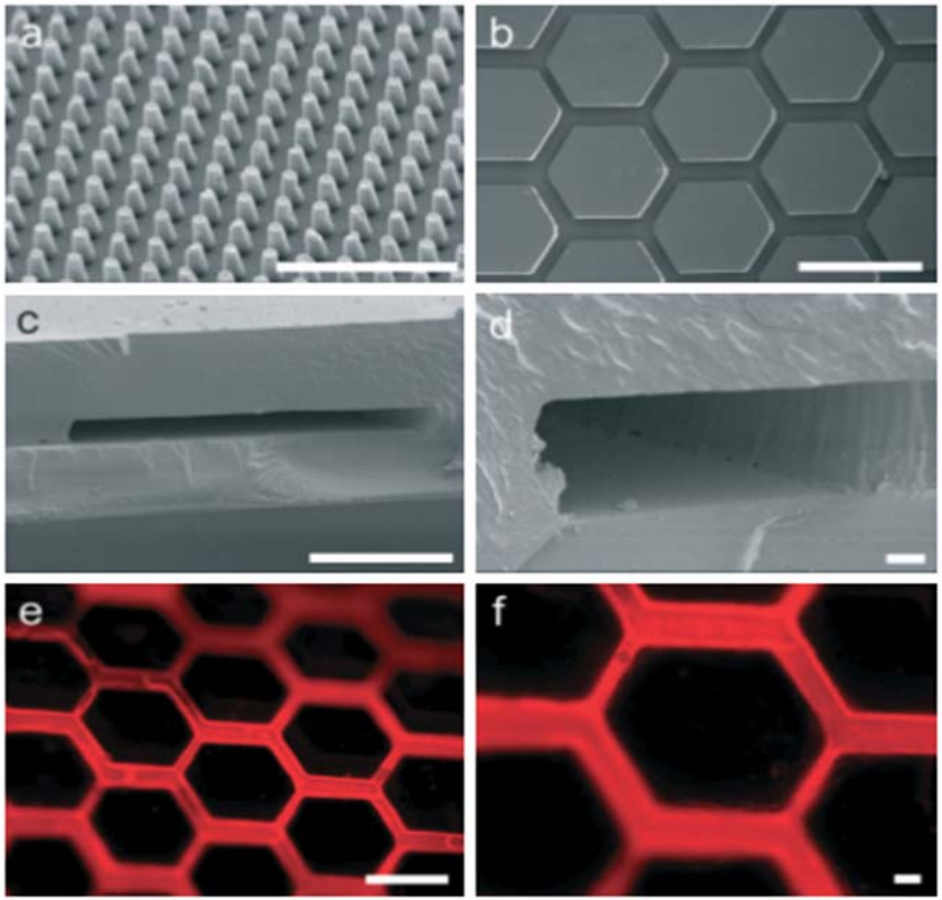

Figure 2. Silk Fibroin-based Microfluidic Devices. Replica molded silk fibroin films produce high-fidelity features including a) nanometer-scale posts with minimum widths of approximately 400 nm and b) micrometer-scale fluidic channels, which were used in subsequent experiments (scale bars are 5 lm and 500 lm in (a) and (b), respectively). c,d) SEM images of the cross-sections of devices fabricated from the strategy outlined in Figure 1 demonstrate retention of feature geometries in thin films with microchannel widths of approximately c) 240 lm and d) 90 lm (scale bars are 200 lm and 10 lm in (c) and (d), respectively). e,f) Patent microfluidic devices are demonstrated by fluorescent micrographs of devices perfused with rhodamine solution. Retention of the perfusate within the microchannels suggests robust bonding at the interface (scale bars are 500 lm and 50 lm in (e) and (f), respectively).

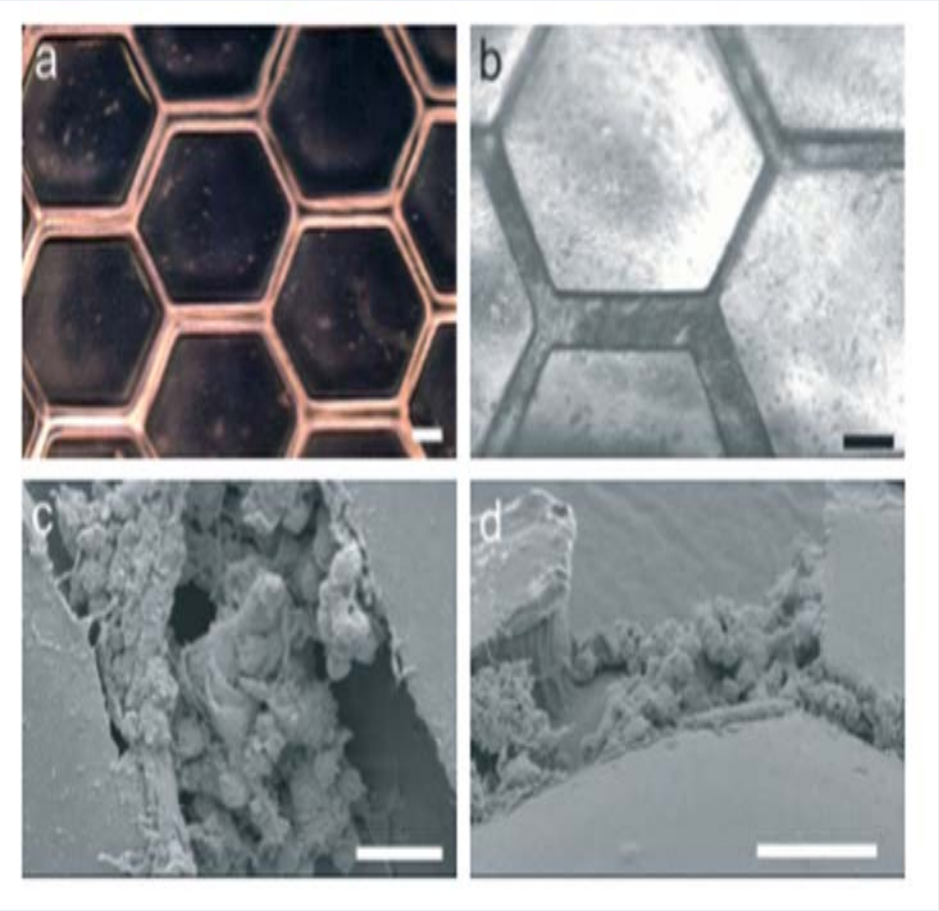

Figure 3. Cell-Seeded Silk Microfluidic Devices. a) Silk microfluidic devices prior to cell seeding are optically clear to permit observation via light microscopy. Hepatocytes were statically seeded for four hours at which time perfusion commenced. b) Devices were partially confluent with cells exhibiting native morphology after 24 h (scale bars are 100 lm in (a) and (b)). c,d) Viable cells remained attached and retained function within devices (see text) for up to 5 d of perfusion as shown in SEM images of sectioned devices (scale bars are 50 lm in (C) and (D)).

✓ Silk micrococoons for protein stabilisation and molecular encapsulation[5]

- 누에에서 추출한 실크는 강도, 탄성 및 생체 적합성을 포함한 고유한 특성을 가짐.
- 실크 피브로인은 용액은 오랜 시간 동안 분산 상태로 오래 가지 못하고 응집이 잘 되는 등의 문제가 있어 이러한 문제를 해결하기 위해 microfluidics-based strategy 를 이용하여 다양한 β-sheet를 포함한 micron-scale capsules를 만들어 특성을 보고함.
- 실크 micrococoons가 효과적인 캡슐화, 저장 그리고 기능화된 antibodies와 같은 응집이 잘되는 단백질의 릴리스 등의 기능을 확인함.
- 실크 micrococoon은 sensitive cargo proteins의 활성을 나타내고 있으며, 활성 생체 분자의 저장 및 방출을 위한 물질임을 확인함.

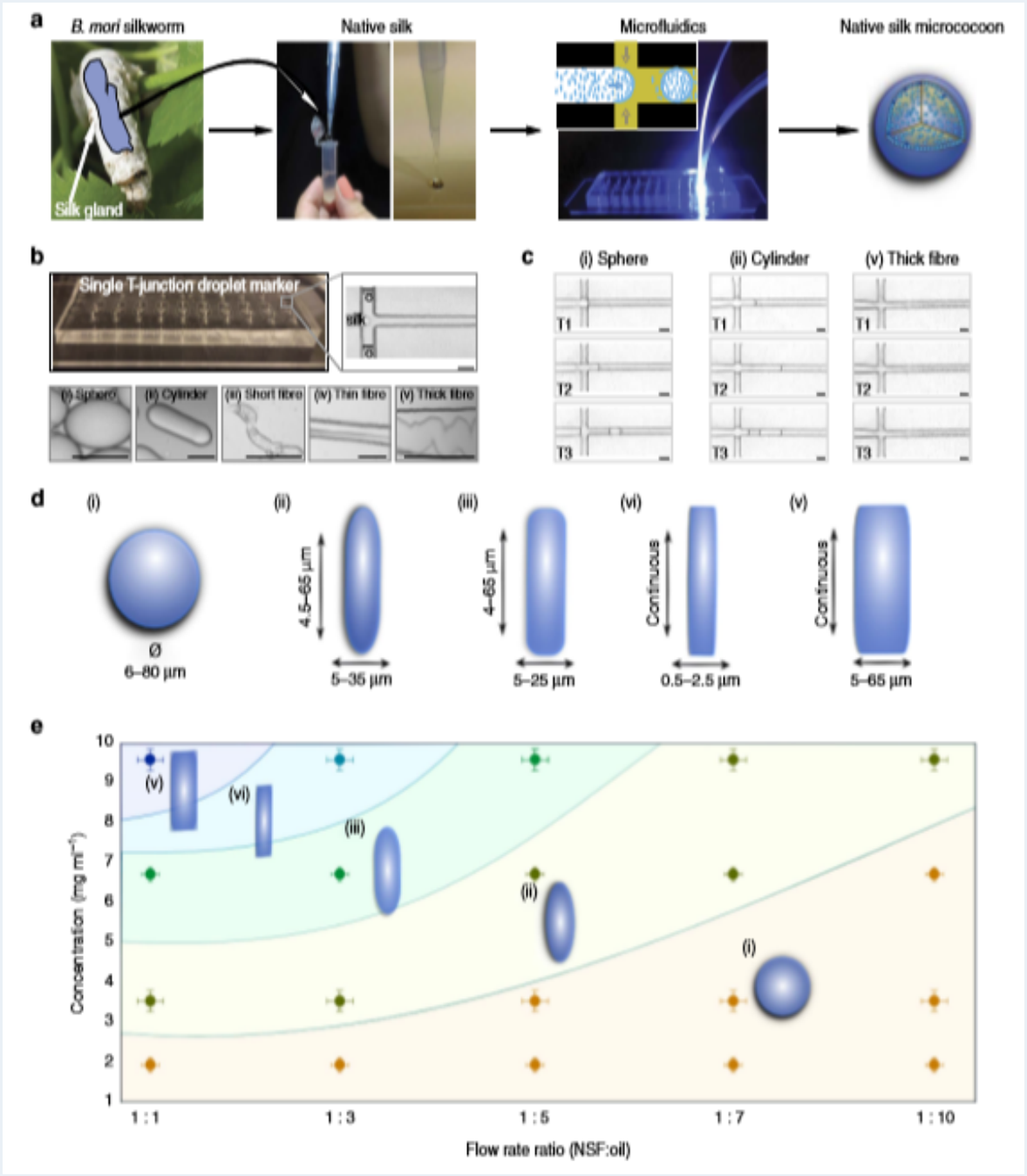

Figure 1 Micrococoon synthesis. (a) Schematic representation of the microfluidic processing of NSF into micrococoons. (b) Optical microscopy images of the NSF micrococoons formed at a single T-junction in the microfluidic device. Micrographs of a variety of NSF micrococoon shapes are shown in the lower panels: (i) sphere, (ii) cylinder, (iii) short fibre, (iv) thin fibre, (v) thick fibre. Scale bar, 20 mm. (c) Micrographs of NSF micrococoon formation acquired at three different time points T1, T2 and T3: (i) sphere; T1¼0 ms, T2¼10 ms, T3¼13 ms, (ii) cylinder; T1¼0 ms, T2¼13 ms and T3¼34 ms and (v) thick fibre; T1¼0 ms, T2¼59 ms, T3¼68 ms. Scale bar, 20 mm. (d) S schematic representations showing the characteristic dimensions of the NSF micrococoons generated in this study. (e) Different micrococoon shapes generated as a function of the protein concentration and of the ratio of the flow rates of the aqueous to oil phases.

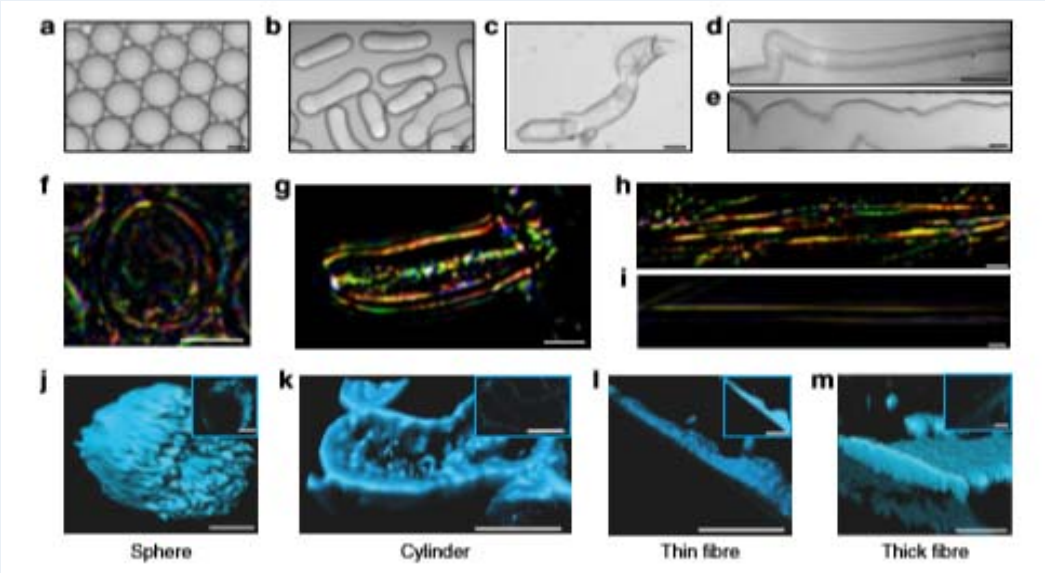

Figure 2 Micrococoon morphology. Bright field microscopy images of NSF micrococoons: (a) spheres, (b) cylinders, (c) short fibres, (d) thin fibres and (e) thick fibres. Scale bar, 5 mm. Images of micrococoon structures placed between crossed polarizers: (f) sphere, (g) cylinder, (h) thick fibre, (i) thin fibre.
Scale bar, 10 mm. 3D reconstructions of confocal images are shown for: (j) a sphere, (k) a cylinder, (l) a thin fibre, (m) a thick fibre. The z-stack central cut images are shown in the inserts. Scale bar, 10 mm.

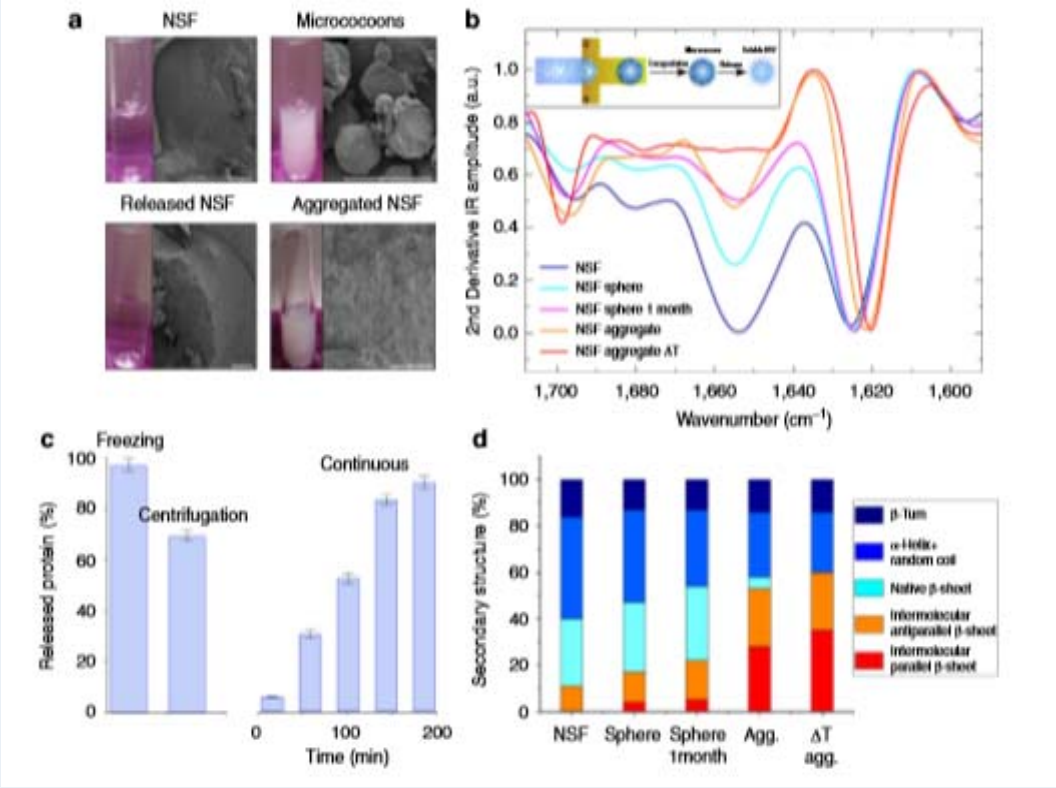

Figure 4 NSF long-term storage and release. (a) Cryo-SEM micrographs showing the morphology of (from left to right) soluble NSF, NSF micrococoons, released and aggregated NSF. Scale bars, 100 mm; The corresponding images of NSF solutions are shown as inserts (left); (b) FTIR spectra of the aggregation and release of NSF by snap-freezing in liquid nitrogen. Insert: schematic representation of the formation of spherical NSF micrococoons and NSF release from micrococoons; (c) histogram showing the efficiency of NSF release by snap-freezing, gentle centrifugation and continuous washing of the NSF micrococoons. The indicated error bars are the s.d. of the average of three different repeats, each one measure 12 times. (d) Histogram of NSF secondary structure elements calculated from the amide I band in the FTIR spectra (b) after release from the microncapsules.

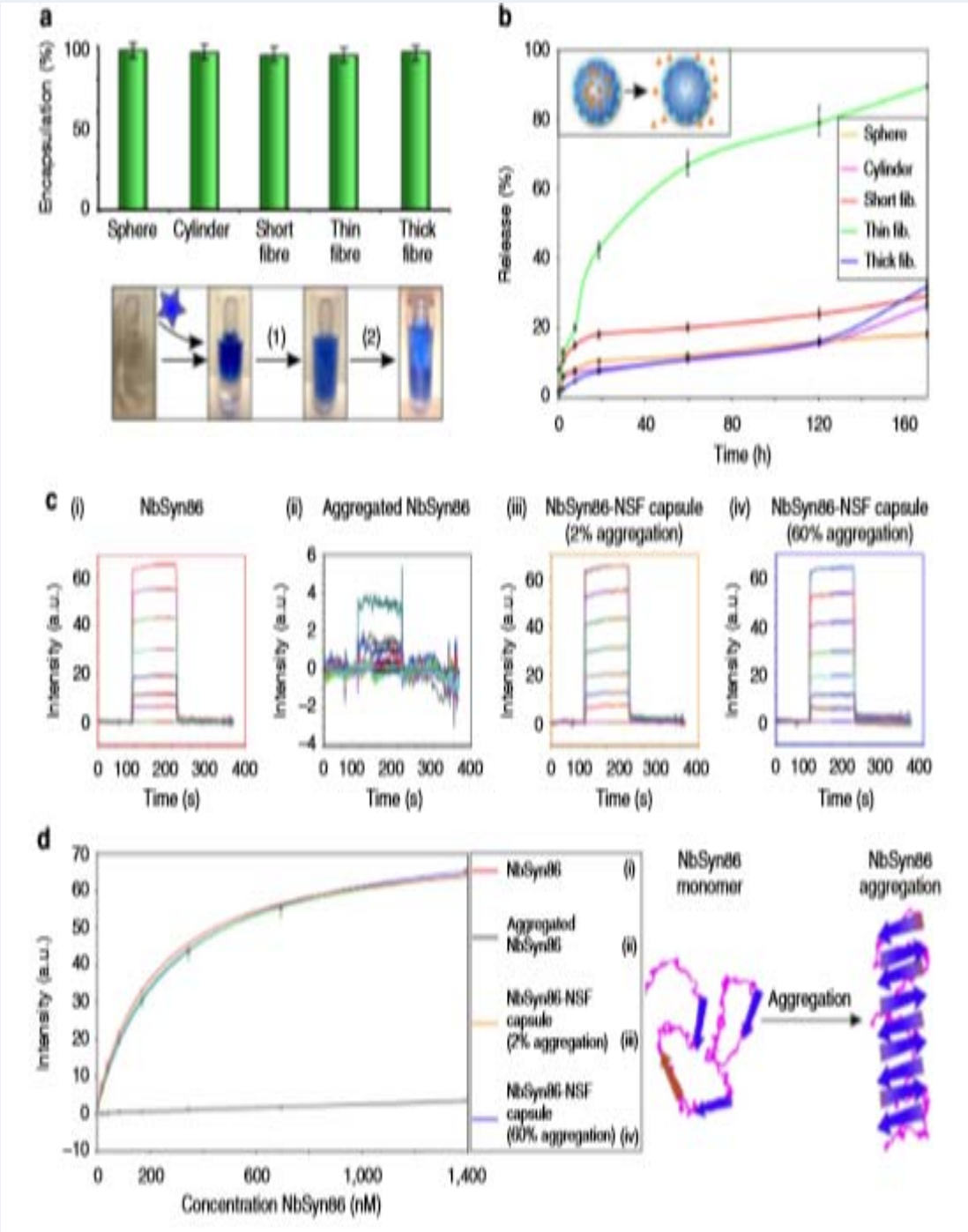

Figure 5 |Antibodies stabilization by encapsulation. (a) Encapsulation efficiency studies for the C4scFv single chain Fv domain in spheres, cylinders, short, thin and thick fibres. The indicated error bars are the s.d. of the average of three different repeats, each one measure 10 times. Insert: schematic representation of the encapsulation and release of antibiody domains by NSF micrococoons: step (1) encapsulation, step (2) release. (b) Release kinetics for C4scFv from different NSF micrococoon shapes. The indicated error bars are the s.d. of the average of three different repeats, each one measure 10 times. (c) Biacore sensorgrams of the binding of NbSyn86 to immobilized a-synuclein: (i) a control sample of monomeric NbSyn86, (ii) NbSyn86 after encapsulation and release treatment in the absence of NSF, (iii) NbSyn86 released from gelled NSF micrococoons (which contain ca. 2% of aggregated NSF), (iv) NbSyn86 released from gelled micrococoons which contain ca. 60% of aggregated NSF. (d) Graph of the equilibrium binding values for the different released NbSyn86 samples (as shown in c) versus the initial (pre-encapsulation) concentration of NbSyn86. The data were fitted to a 1:1 bimolecular binding model to estimate the affinity constant of NbSyn86 for a-synuclein, and were also used to estimate the loss of activity between samples. The indicated error bars are the s.d. of the average of three different repeats, each one measure five times.

3. 결론

- ✓ 마이크로 플루이딕스 디바이스는 물리, 화학, 공학, 생명기술 등 종합적인 기술이 필요한 기술이며 향후 전 분야의 활용 및 산업화가 기대됨.[2]
- ✓ 마이크로 플루이딕스 디바이스의 응용분야는 micro total analysis system, lab-on-a chip, 미세화학반응기, 생물 분석, 셀로 믹스, 약물 전달, 조직 공학 등 광범위하게 적용되고 있음.[2]
- ✓ 향후 마이크로 플루이딕스 디바이스의 연구가 활발하게 보고되고 있으며, 산업화하기 위한 가능성이 기대되는 분야임.[2]

4. 참고 문헌

1. 이경균, 박태정, 이석재, 미세유체 반응 시스템 (Microfluidic Reaction System), *㈜한국바이오칩학회*, **17**, 4(2012)

2. 김도현, 마이크 로플루이딕 시스템의 현황, Korean Chem. Eng. Res., **42**, 375(2004)

3. R. Konwarh, P. Guta, B. B. Mandal. Silk-microfluidics for advanced biotechnological applications; A progressive review, *Biotechnology Advances,* **34**, 845(2016)

4. C. J. Bettinger, K. M. Cyr, A. Matsumoto, R. Langer, J. T. Borenstein and D. L. Kapla, Silk Fibroin Microfluidic Device, *Adv. Mater.,* **19**, 2847(2007)

5. U. Shimanovich, F. S. Ruggeri, E. D. Genst, J. Adamcik, T. P. Barros, D. Porter, T. Mu¨ller, R. Mezzenga, C. M. Dobson, F. Vollrath, C. Holland and T. P. J. Knowles, Silk micrococoons for protein stabilisation and molecular encapsulation, *Nature communications*, **8**, 1(2017)